

# MEASURING BIODYNAMIC FEEDTHROUGH IN HELICOPTERS

(Paper No. 199)

Joost Venrooij<sup>1,2</sup>, Deniz Yilmaz<sup>2</sup>, Marilena D. Pavel<sup>2</sup>,  
Giuseppe Quaranta<sup>3</sup>, Michael Jump<sup>4</sup>, Max Mulder<sup>2</sup>

<sup>1</sup> Max Planck Institute for  
Biological Cybernetics  
Spemannstraße 38, 72076  
Tübingen, Germany

<sup>2</sup> Delft University of  
Technology  
Kluyverweg 1, 2629HS  
Delft, The Netherlands

<sup>3</sup> Politecnico di Milano  
I-20156  
Milano, Italy

<sup>4</sup> University of Liverpool  
Brownlow Hill, L69 3GH  
Liverpool, England

joost.venrooij@tuebingen.mpg.de, d.yilmaz@tudelft.nl, m.d.pavel@tudelft.nl,  
mjump1@liverpool.ac.uk, m.mulder@tudelft.nl

## ABSTRACT

**Biodynamic feedthrough (BDFT) refers to a phenomenon where vehicle accelerations cause involuntary pilot limb motions which, when coupled to a control device, can result in unintentional control inputs. It is known that BDFT occurs in helicopters, amongst many other vehicles. The goal of the current study is to analyze the pilot's response to helicopter motion and experimentally determine the level of BDFT occurring in helicopters.**

**In this study, BDFT was measured for the collective and the cyclic control devices, in roll, pitch, and vertical direction, for three different control tasks, a position task (PT) or 'stiff task', a force task (FT) or 'compliant task', and a relax task (RT). The study focuses on the influence of the pilot's neuromuscular dynamics on the level of BDFT. Two major conclusions can be drawn from the experimental results: 1) BDFT in helicopters is task dependent 2) the highest level of BDFT is measured in lateral direction, followed by longitudinal and finally vertical direction.**

## NOMENCLATURE

APC	Aircraft-pilot couplings
BDFT	Biodynamic feedthrough
CD	Control device
CE	Controlled element
CL	Closed-loop
CNS	Central nervous system
DIR	Disturbance direction
DUT	Delft University of Technology
$F_C$	Contact force [N]
FCS	Flight control system
$F_{dist}$	Force disturbance signal [N]
FP7	7 <sup>th</sup> Framework Programme
FT	Force task
$H_{adm}$	Admittance transfer dynamics
$H_{BDFT}$	BDFT transfer dynamics
HO	Human operator
$I_{HOCD}$	HO-CD interface
$I_{PLFHO}$	PLF-HO interface
LAT	Lateral direction
LNG	Longitudinal direction
$M_{dist}$	Motion disturbance signal [m/s <sup>2</sup> ]
NMS	Neuromuscular system

OL	Open-loop
PAO	Pilot assisted oscillation
PIO	Pilot induced oscillation
PLF	Platform
PT	Position task
RMS	Root-mean-squared
RPC	Rotorcraft-pilot couplings
RT	Relax task
VRT	Vertical direction
$w_f$	Frequency range of force disturbance
$w_m$	Frequency range of motion disturbance
$\Gamma_{adm}$	Squared coherence of admittance
$\Gamma_{BDFT}$	Squared coherence of BDFT
$\theta_{CD}$	Control device deflection [deg]

## 1. INTRODUCTION

Vehicle accelerations and vibrations can degrade pilot manual control performance in various ways [1]. One type of degradation occurs when vehicle accelerations feed through the pilot's body and cause involuntary motions of the limbs. As the pilot is holding the control devices, these involuntary motions of torso, arms and hands cause involuntary control inputs. This phenomenon is called biodynamic feedthrough (BDFT). Biodynamic feedthrough occurs in many different vehicles, such as aircraft, when flying through atmospheric turbulence [2], or during roll-ratcheting. Other examples are heavy hydraulic excavators [3], and electrically powered wheelchairs [4]. Also helicopters suffer from the effects of BDFT [5].

BDFT effects in helicopters have been identified since the beginning of helicopter operations, however, little fundamental research has been undertaken to understand them. As early as 1968 studies were performed into a helicopter related BDFT phenomenon called vertical bounce [6] (also known as collective bounce): a divergent, vertical helicopter oscillation caused by interaction between the vertical motion of the helicopter and the pilot's body, where involuntary motions of the pilot's arm are coupled to the collective pitch stick. Collective bounce usually occurs during transition to or from a hover when the helicopter is at a high gross weight with either an internal or an external load. The authors in [6] mention that 'the presence of the pilot and his thrust lever control' can lead to a 'divergent oscillation' due to the 'pilot's body motion in response to airframe vertical acceleration'.

Pioneering work for a mathematical representation of biomechanical responses was performed in the 1970s [7]-[10]. Examples of the application of these models are the determination of acceptable levels of aircraft aeroservoelastic stability or to assist in the understanding of the so-called aircraft-pilot-couplings (APC) and rotorcraft-pilot couplings (RPC) phenomena [11]. A/RPCs are oscillations or divergent responses of a vehicle originating from adverse pilot-vehicle couplings. These undesirable couplings can range in severity from benign to catastrophic; benign A/RPCs affect the operational effectiveness of a mission, degrading the aircraft handling qualities; catastrophic A/RPCs result in the loss of the aircraft and lives. Until 1995, A/RPCs were usually known under the name of Pilot Induced/Pilot Assisted oscillations (PIO/PAO). PIO occurs when the pilot inadvertently causes divergent oscillations by applying control inputs which are essentially in the wrong direction, or have a significant phase lag with respect to the aircraft/rotorcraft response. PAO is a higher frequency phenomenon related to involuntary control inputs given by the pilot, which may destabilize the aircraft. Biodynamic feedthrough belongs to the class of PAO. The frequencies at which these biomechanical responses occur are crucial to whether a PAO will develop.

In the United States, BDFT investigations relative to RPC phenomena included work done in support of the XV-15, V-22 [12], CH-53E [5][13] and RAH-66 [14]. In Europe, biodynamic tests have been conducted in helicopters during the GARTEUR HC-AG16 project on RPCs [15][16][17]. The experimental campaigns in the GARTEUR project focused on the characterization of the passive behavior of rotorcraft pilots' biodynamics. The results suggested that differences between the pilot's responses on the collective stick due to vertical accelerations can be related to the muscular activation of the pilot's limbs. The same conclusion was drawn on the lateral motion of the cyclic stick.

In the last twenty years, for modern aircraft, it has become increasingly clear that the rapid advance in the field of flight-control-systems (FCS) has increased the sensitivity of the pilot-vehicle system to the appearance of unfavourable A/RPC events [11]. In other words, in the FCS of any modern aircraft, there seems to be some embedded tendencies that predispose the pilot-aircraft system towards A/RPC occurrence. The understanding of pilot BDFT and how it interacts to the aerodynamics, structural dynamics and FCS of the aircraft is of paramount importance to reduce susceptibility to A/RPC occurrences during aircraft development and fleet service. In this context, the European Commission recently launched, under the umbrella of the 7th Framework Programme (FP7), the ARISTOTEL project (Aircraft and Rotorcraft Pilot Couplings – Tools and Techniques for Alleviation and Detection [www.aristotel-project.eu](http://www.aristotel-project.eu)), the aim of which is to advance the state-of-the-art of A/RPC prediction and suppression.

The motivation for studying BDFT effects in helicopters (and other vehicles) is that BDFT causes degradation of control performance which can endanger the comfortable, accurate and, above all, safe operation of vehicles. Despite the attention that BDFT has received over the past years, its fundamentals are only poorly understood. BDFT is a complex phenomenon, with numerous influencing factors and complex interactions [1][7]. It has been shown that the BDFT dynamics depend on factors such as vehicle dynamics, acceleration characteristics (direction, magnitude, frequency content), seating characteristics (seat damping, restraints, armrests) and control device characteristics (type of device, stiffness, damping).

Obviously, the most complex source of influence is undoubtedly the human operator. Not only differences between the body characteristics of different operators (e.g., weight and size) have shown to be of importance [5][18], but also time-varying, more elusive factors such as workload [5] and task interpretation [19]. In other words: BDFT depends on the way the human is interacting with the vehicle. If, for example, a pilot in response to an emergency suddenly stiffens his muscles and increases grip on the control devices, this will alter the way accelerations feed through his body and thus alter the BDFT dynamics.

To understand the influence of neuromuscular dynamics on BDFT a measure is required that 'quantifies' the neuromuscular dynamics. Recently, at Delft University it has been shown that a suitable property to quantify the neuromuscular dynamics in BDFT studies is the neuromuscular admittance [20]. Neuromuscular admittance (or shortly admittance) describes pilot limb dynamics as the dynamical relationship between force input and position output. The admittance contains the effect of both static features (e.g., limb weight) and time-varying features (e.g., muscle co-contraction). Admittance can be interpreted as the 'mechanical dynamics' of the human operator's limb as he/she interacts with the control device. This makes neuromuscular admittance an insightful instrument in understanding BDFT.

The goal of the current paper is to investigate BDFT effects in helicopters. BDFT was measured in an experiment conducted in the SIMONA motion-based simulator at Delft University of Technology (DUT) [21] using a helicopter setup. The methodology for measuring BDFT in helicopters is based on a general method to measure BDFT, extensively described in [20]. During the experiment the BDFT and neuromuscular admittance were measured simultaneously for three different control tasks, i.e. a position task (PT) or 'stiff task', a force task (FT) or 'compliant task', and a relax task (RT). Each control task required a different setting of the neuromuscular system, leading to different admittance and BDFT dynamics for each task. Measurements were performed using cyclic stick in lateral (left-right) and longitudinal (forward-backward) directions and collective stick in vertical (up-down) direction. The present paper reveals the analysis of these experimental results, focusing on 1) the influence of the pilot's neuromuscular dynamics on BDFT and 2) the influence of the disturbance direction on BDFT.

## 2. BIODYNAMIC FEEDTHROUGH SYSTEM MODEL

A generic biodynamic feedthrough system model will be proposed in the following. This model helps to understand the different elements that play a role in BDFT. The model is described in more detail in [20].

Considering helicopter control on a system level, one can distinguish several elements: the pilot, the helicopter and the control devices (cyclic and collective). To represent the BDFT problem in a generic sense, in the following these elements will be called the human operator (HO), the controlled element (CE) and the control devices (CD), respectively. These elements and their interconnection are indicated in black in Fig. 1.

The HO is controlling the (partial) state of the CE by comparing the current state  $Y_{cur}$  with a certain goal state  $Y_{goal}$ . The CE can be disturbed by a disturbance signal, for which the HO is requested to compensate. The HO can influence the state of the CE by means of the CD. Control commands are applied by exerting a force, the contact force  $F_C$ , on the CD, resulting in a control device deflection,  $\theta_{CD}$ , which in turn enters the CE.

The HO model can be split into the central nervous system (CNS), and the neuromuscular system (NMS). The CNS is responsible for monitoring the state of the CE and generating all cognitive control commands. These commands are neurally communicated to the NMS. The NMS represents the neuromuscular system of the limb connected to the control device and contains body elements such as bones, muscles, etc. The dynamics contained in the NMS are described by the neuromuscular admittance. In this study, the neuromuscular admittance was measured using a force disturbance signal that was inserted in the control device (as will be detailed in the Section 4). This force disturbance signal,  $F_{dist}$ , is indicated in Fig. 1 in gray. Note that  $F_{dist}$  is not part of the BDFT problem but used only to measure the neuromuscular admittance.

Next, the model of Fig. 1 can be extended to include BDFT effects, by adding the effect of vehicle accelerations. Two types of BDFT systems can be distinguished: ‘open-loop’ (OL) and ‘closed-loop’ (CL); the difference being whether or not the operator’s control actions influence the vehicle accelerations. In case of the helicopter pilot, the BDFT system is closed-loop: the pilot has a direct influence on the accelerations he/she is subjected to. However, other occupants on board of the helicopter might experience involuntary limb motion due to the helicopter motion as well, while executing control over any CE other than the helicopter (e.g. when pointing a camera). That type of BDFT system is called open-loop.

The existence of two types of BDFT systems is the prime reason to include an extra model block, the platform (PLF). The PLF block contains the vehicle motion dynamics and its output is the actual source of BDFT problems: vehicle accelerations. The vehicle acceleration signal is called  $M_{dist}$ . Open-loop and closed-loop BDFT systems are implemented in the model using a switch, as shown in Fig. 1. In case of BDFT in helicopters, for each occupant of a helicopter the PLF dynamics are the same, the CE may differ, but only for the pilot the BDFT system

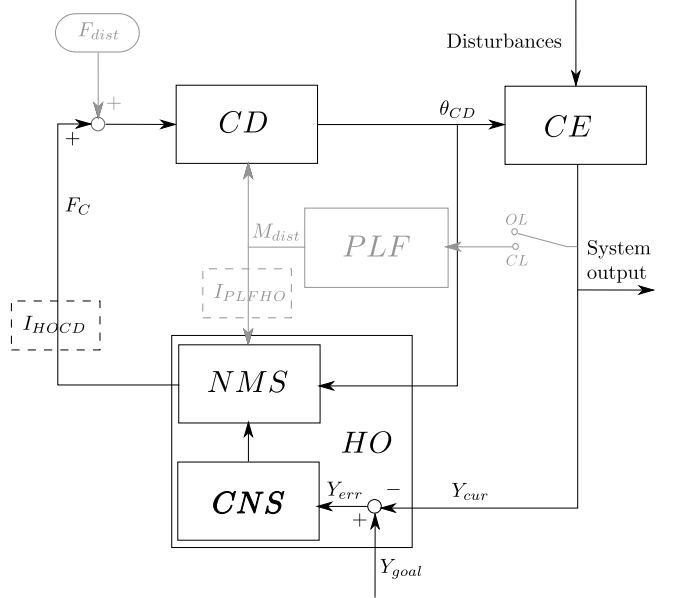


Figure 1: generic biodynamic feedthrough system model

is closed-loop, where the switch closes the loop between control inputs and vehicle motion.

The feedthrough of PLF accelerations via the body of the HO into the CD is governed by two ‘interfaces’. These interfaces describe the dynamics between the human operator and the environment and are shown in Fig. 1 by the dashed boxes,  $I_{PLFHO}$  and  $I_{HOCD}$ . The interface  $I_{PLFHO}$  describes the dynamics of the connection between the PLF and the HO, e.g., seat damping or the effect of seat belts. Its dynamics determine how accelerations enter the body of the operator. The interface  $I_{HOCD}$  describes the dynamics of the connection between HO and CD, e.g., grip viscoelasticity or the effect of an arm rest. This interface determines how limb motions result in contact forces  $F_C$ .

Which part of Fig. 1 describes BDFT, the phenomenon of interest in this study? In essence, BDFT is the influence of the motion signal  $M_{dist}$  on the contact force  $F_C$  and consequentially on the control device deflections  $\theta_{CD}$ . Taking all relevant sources into account, it follows that the control input signal  $\theta_{CD}$  consists of several contributions:

$$\theta_{CD}(t) = \theta_{CD}^{cog}(t) + \theta_{CD}^{F_{dist}}(t) + \theta_{CD}^{M_{dist}}(t) + \theta_{CD}^{rem}(t),$$

where the superscript *cog* denotes the cognitive element in the control device deflection, i.e., the part that is due to voluntary control actions coming from the CNS. The superscript  $F_{dist}$  denotes the contribution of the force disturbance and  $M_{dist}$  the contribution of the motion disturbance. The remaining part of the input, the remnant, is denoted with the superscript *rem*. Remnant can be defined as the pilot’s control output power that is not linearly correlated with the system input. As linearity is assumed in the analysis, the remnant should be small. This assumption can be checked using the squared coherence, which is a measure for the linearity of the measured response (see Section 4.7). The contact force  $F_C$  is composed of the same contributions:

$$F_C(t) = F_C^{cog}(t) + F_C^{F_{dist}}(t) + F_C^{M_{dist}}(t) + F_C^{rem}(t).$$

BDFT is the effect where motion accelerations  $M_{dist}$  enter the NMS, leading to involuntary contact forces, which enter the CD, yielding involuntary control device deflections  $\theta_{CD}^{M_{dist}}$ , or:

$$M_{dist} \rightarrow H_{BDFT}(s) \rightarrow \theta_{CD}^{M_{dist}}$$

where  $H_{BDFT}(s)$  stands for the BDFT transfer function.

### 3. MEASURING BIODYNAMIC FEEDTHROUGH IN HELICOPTERS

As it is the goal of this paper to investigate BDFT effects in helicopters, it might appear to be most straightforward to implement a high-fidelity helicopter model on a motion simulator and study closed-loop BDFT effects using helicopter pilots as subjects. This is, however, not the approach taken in this study. Instead, it will be argued that by investigating BDFT effects in an open-loop fashion equally valuable and possibly more widely applicable results may be obtained. In this study the SIMONA simulator motion base was used as a three axis shake-base, and ‘global’ BDFT measurements were performed instead of helicopter specific mission tasks.

The transfer dynamics between  $M_{dist}$  and  $\theta_{CD}^{M_{dist}}$ , i.e., the BDFT dynamics, are studied in the frequency domain, resulting in Bode plots showing the BDFT dynamics for a range of frequencies. The range for which the BDFT dynamics can be determined depends completely on the disturbance signal  $M_{dist}$ : BDFT dynamics can only be determined for frequencies where the  $M_{dist}$  signal contains sufficient power. One could either use a ‘specific’ disturbance signal, representative for the accelerations felt in a specific helicopter (e.g., a BO-105) in a certain condition (e.g., cruise), or a generic ‘broad’ disturbance signal, containing a broad frequency spectrum, which are not specific to a particular vehicle or condition. The effect that the type of disturbance signal (‘specific’ or ‘broad’) has on the resulting BDFT estimate is illustrated in Fig. 2. As a ‘specific’ disturbance signal only contains power on a limited number of frequencies, the BDFT estimate can only be determined on these frequencies, yielding a very ‘sparse’ estimate. A ‘broad’ disturbance signal, however, contains power on a large range of frequencies, yielding a more complete estimate. When the goal is to study BDFT in a very specific environment, in which the accelerations

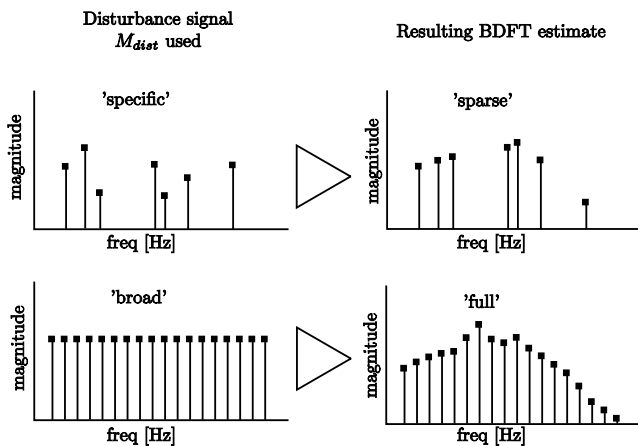


Figure 2: result when using a ‘specific’ or ‘broad’ disturbance signal



Figure 3: SIMONA Research Simulator

have a well defined frequency spectrum, the ‘specific’ disturbance signal may yield more accurate results, but at the price of a limited applicability. If the disturbance situation under investigation is less clearly defined (which is the case in this particular study), the ‘full’ estimate is preferred with regard to the information quantity and applicability of the results. However, one might question how can one relate the ‘full’ BDFT spectrum to a specific helicopter situation? Once the ‘full’ BDFT dynamics are obtained, the BDFT effects occurring in a specific condition (e.g., cruise in a BO-105) can be *calculated* using a representative motion disturbance, specific to the situation under investigation, and employing the ‘full’ BDFT estimate as transfer dynamics model. Therefore, the authors argue that using the ‘broad’ spectrum, although not specific to any helicopter or situation, yields valuable and insightful results.

The above discussion implies that the approach adopted in this paper is an open-loop approach where one does not define the dynamics in the CE block or the PLF block, but define  $M_{dist}$  directly. What remains as a necessity to make the BDFT measurements applicable to helicopters is the use of helicopter cabin elements as seat, seat belts and a cyclic and collective as control interfaces.

In summary, measuring broad spectrum, generic BDFT effects in helicopters can be achieved by meeting the following requirements:

1. [ $M_{dist}$  magnitude] Supplying a sufficiently strong motion disturbance signal  $M_{dist}$ , such that the NMS of the human operator is sufficiently perturbed to cause significant BDFT effects
2. [ $M_{dist}$  freq. content] Supplying a sufficiently rich motion disturbance signal  $M_{dist}$ , such that BDFT can be studied for a relevant range of frequencies.
3. [ $\theta_{CD}^{M_{dist}}$  separation] Designing the disturbance signal and control task such that the contribution of the motion disturbance signal on the control device deflection (i.e.,  $\theta_{CD}^{M_{dist}}$ ) can be determined.
4. [helicopter elements] Use an experimental setup containing realistic helicopter cabin elements, which are of influence on the BDFT dynamics, such as seat and seatbelts, control device location and dynamics. The adjustment of seat and seat belts should be the same across subjects.

### 4. METHODS

The experimental setup was developed by adapting a more general method, extensively described in [20].

Table 1:  
Data of subjects (N=14)

	Age (years)	Weight (kg)	Length (cm)	BMI (kg/m <sup>2</sup> )
Mean	29.3	76.4	179.7	23.6
STD	5.7	13.3	6.9	3.0
Range	23-43	58-105	167-190	19.9-29.9

#### 4.1 APPARATUS

The experiment was performed on the SIMONA Research Simulator of Delft University of Technology, a six degree-of-freedom flight simulator [21] (Fig. 3). The control devices were electrically actuated collective and cyclic controls with adjustable dynamics settings. These settings were duplicated from the rotorcraft handling qualities research experiments conducted by Mitchell et al. [22]. The settings of these control devices were kept constant during the experiment. The seat in which the subjects were seated had a 5-point safety belt that was adjusted tightly.

#### 4.2 SUBJECTS

Fourteen subjects (11 males, 3 females) participated in the experiment. The subjects were volunteers from the Delft University of Technology. See Table 1 for the subject data.

#### 4.3 EXPERIMENT DESIGN

The subjects performed three different disturbance-rejection tasks [23]: a *position task* (PT) or 'stiff task', with the instruction to minimize the position of stick, i.e., 'resist forces', a *force task* (FT) or 'compliant task', with the instruction to minimize the force applied to the stick, i.e., 'yield to forces', and a *relax task* (RT), with the instruction to relax the arm, i.e., 'ignore forces'. The human operator needed to set his/her neuromuscular properties differently for optimal control of each of the three control tasks. The PT required a maximum stiffness of the NMS, where the FT required a minimum stiffness. Note that the RT is a passive task, resulting in a stiffness level between the one found in the PT and FT. By using these three task instructions, the effect of maximum neuromuscular adaptation on BDFT can be investigated.

During the execution of the tasks, two disturbance signals were used simultaneously: the force disturbance  $F_{dist}$ , which perturbed the control device, and the motion disturbance  $M_{dist}$ , which perturbed the simulator, inducing BDFT. With  $F_{dist}$  the neuromuscular admittance was determined, with  $M_{dist}$  biodynamic feedthrough was measured. The force disturbance consisted of a force signal, applied to a single axis of the control device. The motion disturbance consisted of a translational acceleration signal, applied to a single axis of the simulator. The measurements were performed for three disturbance directions (DIR): lateral (LAT), longitudinal (LNG) and vertical (VRT). The directions of  $F_{dist}$  and  $M_{dist}$  were always aligned with the disturbance direction. Together with the three tasks (TASK) this results in 3x3 conditions:

- TASK: PT, RT, FT
- DIR: LAT, LNG, VRT

Each condition was repeated 6 times.

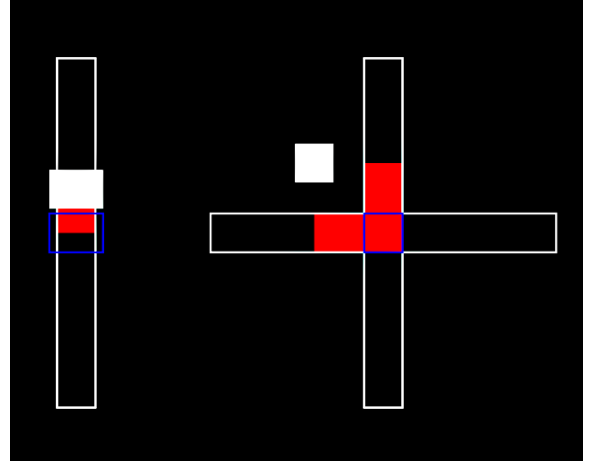


Figure 4: experimental display. Left shows collective, right shows cyclic (roll in horizontal and pitch in vertical). The figure shows collective slightly above target value of 50%. Cyclic is slightly deflected to the left and forward.

#### 4.4 PROCEDURE

Before entering the simulator the subjects were instructed on the goal of the experiment and the control tasks they were to perform. Inside the simulator, the subjects were strapped in the seat and instructed on the use of the control devices. Performance information was displayed on a 15" LCD screen in front of the subject during the execution of the task.

During the position task the display showed the positions of the three control axes: an up-down moving square showed the position of the collective, an up-down and left-right moving square showed the position of respectively the pitch and roll axis of the cyclic (see Fig. 4). Blue squares indicated the target value for each axis: both cyclic axes at 0 degrees (centered) and collective at 50%. During the force task the display showed the force applied in each control axis against the target force ( $0 N$  for each axis). During the RT no performance feedback was provided, as this task has no reference value in either force or position. The subjects were asked to keep all control devices at the target position or force as well as they could, but to put focus on the axis that was being perturbed. After each run the subjects were presented with a score as a measure of their performance. Several training runs were performed, first without the simulator moving, to allow the subject to get used to the force disturbances and the different control tasks. When a consistent performance (i.e., score) was reached, the actual measurement started.

Six repetitions of each control task (PT, FT, RT) were performed in each direction (LAT, LNG, VRT), resulting in 6x3x3 experiment runs. All tasks in a disturbance direction were grouped, and the directions offered in random order. The tasks were performed in groups of two tasks, e.g., two PT's followed by two RT's, etc. The order of the task groups was random.

#### 4.5 DISTURBANCE SIGNAL DESIGN

Both disturbance signals,  $F_{dist}$  and  $M_{dist}$ , were multi-sines, defined in the frequency domain. The signals were separated in frequency to allow distinguishing the response due to each disturbance in the measured signals [23]. Fig. 5 shows the power spectral density plot of the disturbance signals used in the PT-LAT condition. The frequency

Table 2:  
Disturbance signal RMS and gains

		F <sub>dist</sub> (N)			M <sub>dist</sub> (m/s <sup>2</sup> )		
		PT	RT	FT	PT	RT	FT
LAT	RMS	20.4	2.09	1.85	0.95	0.74	0.74
	Gain	30	2.9	2.5	0.9	0.7	0.7
LNG	RMS	47.7	2.73	2.5	0.95	0.74	0.74
	Gain	70	3.35	3.3	0.9	0.7	0.7
VRT	RMS	67.86	2.32	2.15	0.6	0.6	0.6
	Gain	100	3	3	0.9	0.9	0.9

content of the disturbance signals was equal in all conditions, only the magnitude varied. The magnitude was varied in such a way that the standard deviation of the control device deflections was approximately similar in each condition to allow comparison across conditions [20]. Due to the different control tasks and directions, the force and motion disturbance gains needed to be tuned for each condition. The results of this tuning procedure are shown in Table 2, where the root-mean-squared (RMS) value and the associated gains are listed for both disturbance signals for each condition.

To obtain a full bandwidth estimate of the admittance, a range between 0.05 Hz and 21.5 Hz was selected for the force disturbance signal  $F_{dist}$ . This is a sufficient bandwidth to capture all arm dynamics [24]. For the motion disturbance signal  $M_{dist}$ , a range between 0.1 and 21.5 Hz was selected. For both disturbance signals, 31 logarithmically spaced frequency points were selected in the frequency range, without overlap between the two disturbance signals. To allow for frequency averaging, power was applied to two adjacent frequency points for each point [25], yielding 31 pairs of frequency points (i.e., 62 points) for each disturbance signal.

Due to the large number of rotating components, assemblies, transmission systems, and the aero-elastic modes of the rotorcraft fuselage, tail boom and rotors, a helicopter pilot is subjected to a wide range of acceleration frequencies [26]. It was assumed that the 31 frequency pairs between 0.1 and 21.5 Hz cover the range of the frequencies where relevant BDFT effects occur. Generally, it is considered that pilot biomechanical responses may affect flexible or structural mode frequencies up to 10 Hz, independent of axis [27].

Table 3:  
Rotor mode priority on response channel (from [19]) with the corresponding frequencies obtained from Bo-105 simulation model

		Response channel			Freq. (Hz)
		Longitudinal	Lateral	Heave	
Flap	Advancing	Medium priority	Medium priority	Low priority	14.68
	Coning	Low priority	Low priority	<b>High priority</b>	<b>7.59</b>
	Regressive	Medium priority	Medium priority	Low priority	0.50
Lead-Lag	Progressive	<b>High priority</b>	<b>High priority</b>	Low priority	<b>11.19</b>
	Coning	Low priority	Low priority	Low priority	4.12
	Regressive	<b>High priority</b>	<b>High priority</b>	Low priority	<b>2.96</b>

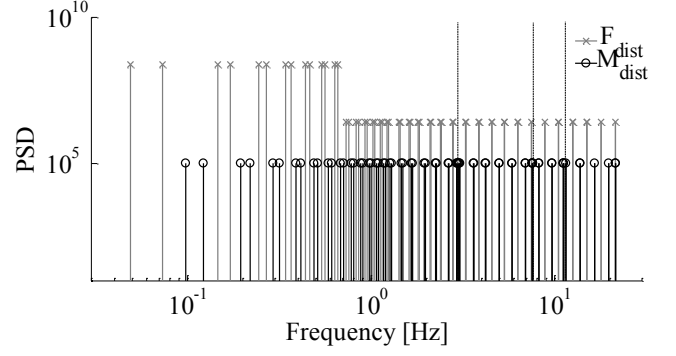


Figure 5: Power spectral density of disturbance signals

When studying helicopters, the rotor modes are of special importance. In [28] the effective rotor modes on particular response axes were identified. The result of the study is summarized in the Table 3 by representing `High`, `Medium` and `Low` priorities. In addition, using an analytical Bo-105 simulation model the corresponding frequencies were calculated and are also shown in Table 3. In this model a generic lag damper was included in the rotor model, and blade flexibility was ignored (in accordance with [29]). To investigate the effect of rotor modes, the motion disturbance signal  $M_{dist}$  was `enriched` to contain frequencies for three important rotor modes with the highest priorities: lag regressive mode (~2.96 Hz), the lag progressive mode (~11.19 Hz), and flap coning mode (~7.59 Hz), which have dominant effects on longitudinal and lateral, and heave motion, respectively. Note that several other modes such as 1<sup>st</sup> fuselage modes (tail boom), transmission, engine modes, etc. were also covered by the disturbance frequency bandwidth (0.1 and 21.5 Hz), but no extra frequencies were added to study them in detail. The location where the three additional groups of frequencies were added is indicated in Fig. 5 by three extended vertical lines. For each mode, the two nearest frequency pairs (i.e., 4 points) were selected, resulting in 12 extra frequency points in total. Adding these frequencies to the motion disturbance signal allows for studying the BDFT effects in detail at these rotor modes.

In the analysis the results were calculated for each available frequency point, (62 points for  $F_{dist}$ , 74 points for  $M_{dist}$ ) and then averaged for each pair resulting in 31 points for  $F_{dist}$  and 37 data points for  $M_{dist}$ . The procedure of averaging increases the reliability of the results [25].

The phase of the sine components was randomized in order to obtain an unpredictable signal. To allow estimation of full-bandwidth dynamics, without influencing the low-frequency behavior, the reduced power method [30] was used to construct the force disturbance signal  $F_{dist}$  (see Fig. 5).

#### 4.6 RECORDINGS

During the experiments the angular deflection of the side-stick  $\theta_{CD}$ , and the applied force to the side-stick  $F_C$  were measured. The disturbance signals were recorded.

#### 4.7 NON-PARAMETRIC IDENTIFICATION

The admittance was estimated in the frequency domain, using a closed loop identification technique using the estimated cross-spectral density between  $F_{dist}$  and  $\theta_{CD}$  ( $\hat{S}_{fd-\theta}(w_f)$ ) and the estimated cross-spectral density between  $F_{dist}$  and  $F_C$  ( $\hat{S}_{fd-f}(w_f)$ ) [31]:

$$\hat{H}_{adm}(w_f) = \frac{\hat{S}_{fd-\theta}(w_f)}{\hat{S}_{fd-f}(w_f)},$$

where  $w_f$  is the frequency range of the force disturbance signal  $F_{dist}$ . The procedure to calculate neuromuscular admittance assumes linearity. To check the reliability of this assumption the squared coherence was calculated:

$$\hat{\Gamma}_{adm}(w_f) = \frac{|\hat{S}_{fd-\theta}(w_f)|^2}{\hat{S}_{fd-fd}(w_f)\hat{S}_{\theta-\theta}(w_f)}.$$

Squared coherence is a measure for the signal to noise ratio and thus for the linearity of the dynamic process. This function equals one when there are no non-linearities and no time-varying behavior and zero when there is no linear behavior at all.

In a very similar way the transfer function describing the biodynamic feedthrough dynamics  $H_{BDFT}$  can be estimated. The estimate of the biodynamic feedthrough dynamics, is calculated using the estimated cross-spectral density between  $M_{dist}$  and  $\theta_{CD}$  ( $\hat{S}_{md-\theta}(w_m)$ ) and the estimated auto-spectral density of  $M_{dist}$  ( $\hat{S}_{md-md}(w_m)$ ):

$$\hat{H}_{BDFT}(w_m) = \frac{\hat{S}_{md-\theta}(w_m)}{\hat{S}_{md-md}(w_m)},$$

where  $w_m$  is the frequency range of the motion disturbance signal  $M_{dist}$ . The squared coherence function for this case:

$$\hat{\Gamma}_{BDFT}(w_m) = \frac{|\hat{S}_{md-\theta}(w_m)|^2}{\hat{S}_{md-md}(w_m)\hat{S}_{\theta-\theta}(w_m)}.$$

## 5. RESULTS AND DISCUSSION

Fig. 6 shows the magnitude, phase and coherence of the admittance measured for a typical subject for the longitudinal direction. The thick lines indicate the mean over the 6 repetitions of each control task; the bands indicate the standard deviation. The high squared coherence values (close to 1) indicate that the dynamics have a high degree of linearity and the estimate is reliable. It can be observed that a clear difference in neuromuscular admittance was achieved by the execution of the three different tasks. The admittance for the PT is low, signifying a small position change due to a force disturbance ('stiff' behavior), where the admittance for the FT is high, signifying a large position change due to a force disturbance ('compliant' behavior). The admittance measured for the RT lies between the ones measured for the PT and FT, as expected. The results in other disturbance directions showed similar features. The results of other subjects were also comparable. The admittance results obtained here are comparable to the ones found in other studies [31][20][23].

As was also observed in [20], some subjects showed only little difference between the RT and FT, in particular for the lateral direction. In [20] this was attributed to an inappropriate force scaling or a failure to instruct the subject clearly enough on the difference between the RT and FT task. In this experiment, it became clear, however, that most of the subjects which showed little difference between RT and FT in the lateral direction, did show differences in admittance in other directions, which indicates that the tasks were properly understood.

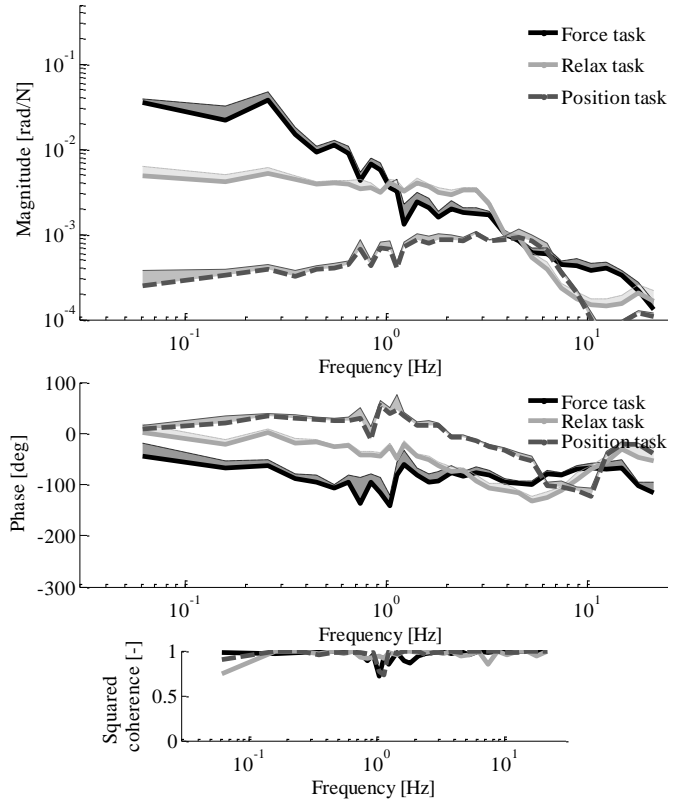


Figure 6: Admittance of a typical subject in longitudinal direction, averaged over 6 repetitions

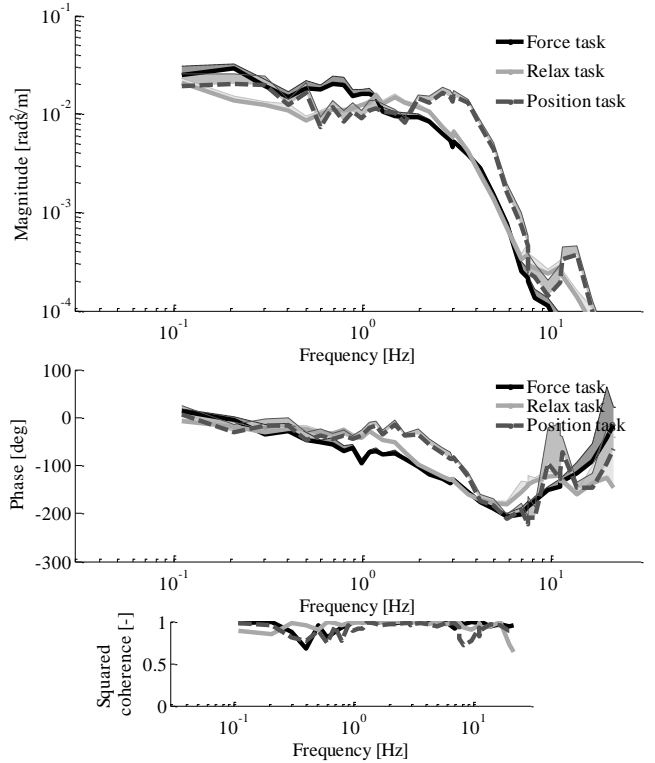


Figure 7: BDFT for a typical subject in longitudinal direction,

Currently, the hypothesis that gravity effects are influencing (increasing) the admittance estimate, especially during the RT in the lateral direction, is being investigated. The results will be published in future publications. Only two subjects showed no significant difference between admittance in FT and RT in any direction. It is possible that these subjects failed to understand or execute the tasks properly; therefore these subjects were excluded from the further analysis, leaving 12 subjects for analysis.

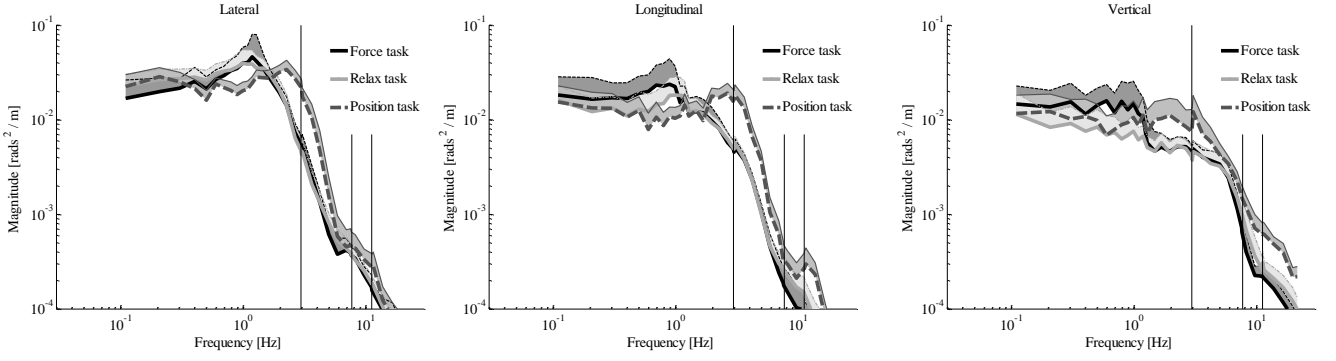


Figure 8: BDFT averaged over all subjects, the result of each task is shown for each direction

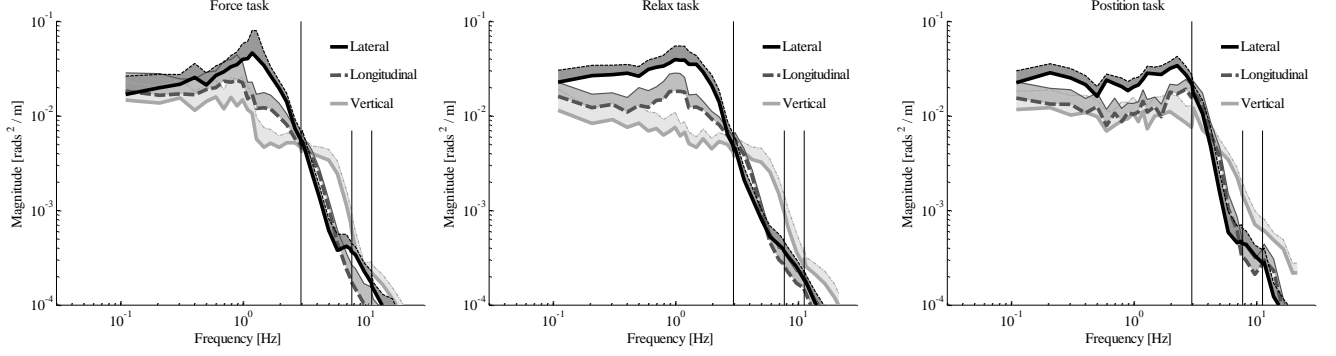


Figure 9: BDFT averaged over all subjects, the result direction is shown for each task (note that the data presented is identical to Fig. 8, but now grouped per task)

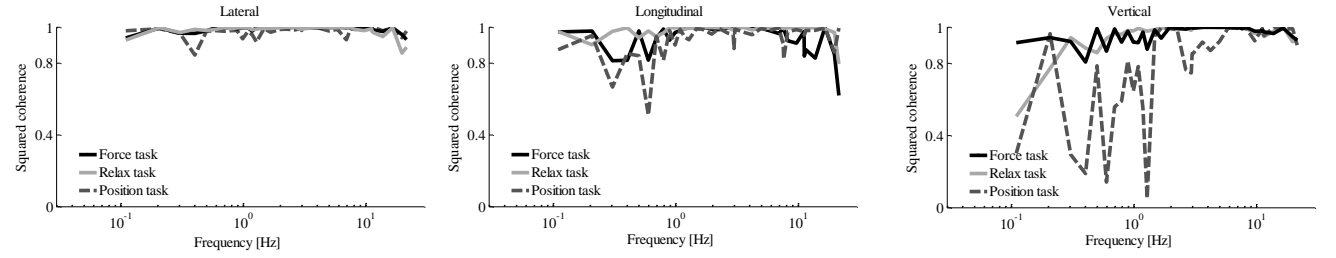


Figure 10: Squared coherences of BDFT measurements in each direction

Fig. 7 shows the magnitude, phase and coherence of the BDFT measured for the same subject and direction (longitudinal) as shown in Fig. 6. The thick lines indicate the mean over the 6 repetitions of each control task; the bands indicate the standard deviation. The high squared coherence values indicate that the dynamics have a high degree of linearity and the estimate is reliable. Standard deviations are only small, indicating that the results are repeatable. Although the absolute differences in magnitude and phase are smaller between the different tasks than for the admittance, it can be observed that the level of BDFT differs from task to task, something that was also found in [19] and has been attributed to changes in neuromuscular admittance. Across subjects, the BDFT level measured for a particular task differed slightly, but shared similar features. The difference observed across subjects is labeled inter-subject variability; the differences observed for a single subject (between tasks) is labeled intra-subject variability.

In the remainder of the paper only the average BDFT magnitude, calculated over all subjects will be discussed. Fig. 8 shows the BDFT magnitude, as averaged over all 12 subjects, for each condition, grouped per disturbance direction. Fig. 9 shows the same data, but now grouped per

task. From Fig. 8 it follows that the task dependency, already observed for one subject in Fig. 7, does not only show in the longitudinal direction but in each of the disturbance directions. Especially the BDFT measured during the PT differs from the one measured during the RT or FT, but also between the latter two tasks differences can be observed. This implies that the level of BDFT depends on the neuromuscular setting of the human operator. More particularly, it can be observed that for all three directions, for disturbances above 1-2 Hz, the PT results in the highest level of BDFT. For this task, also a peak in the BDFT level can be observed between approximately 2 and 3 HZ for each direction. This implies that ‘stiff’ behavior, although largely beneficial at lower frequencies, is the worst strategy when dealing with motion disturbances above 1-2 Hz. Similar observations were made in [20], where BDFT was measured in lateral direction for the same tasks with a side-stick.<sup>1</sup> From Fig. 9 one can see that

<sup>1</sup> In comparison with [20], the results of the present study show a BDFT level that is significantly lower. This can be attributed to the difference in control device dynamics. The mechanical impedance of the collective and cyclic were set to be higher (resulting in a ‘heavier’ stick) than that of the side-stick used in [20]. It is known that higher mechanical impedance reduces BDFT as the same applied force results in a smaller stick deviation [1].

BDFT is also depending on the disturbance direction. For the lower frequencies, up to 3-4 Hz, the level of BDFT is the highest in the lateral direction and the lowest in the vertical direction. From disturbances of 3-4 Hz and up the BDFT is the highest in the vertical direction. As the feedthrough at lower frequency results in inputs of larger amplitude it can be concluded that, overall, the level of BDFT is highest in lateral direction, followed by longitudinal and finally vertical direction.

The vertical lines in Fig. 8 and Fig. 9 indicate the locations of the three rotor modes that were selected for more detailed study: the lag regressive mode (~2.96 Hz), flap coning mode (~7.56 Hz), and the lag progressive mode (~11.19 Hz). The disturbance signal was 'enriched' to provide an accurate BDFT estimate around these modes. Several observations can be made for the level of BDFT at these frequencies.

For each of the modes, the BDFT is the highest during the PT. The lag regressive mode seems to coincide with the peak in BDFT that occurs for this task around 2-3 Hz. In addition, at approximately 11 Hz, i.e., the frequency close to that of the lag progressive mode, the BDFT dynamics show a peak during the lateral position task. Also a smaller bump can be observed at this frequency for this task in the lateral direction. Note that this frequency lies outside of the range where a pilot can generate cognitive control inputs. The observations above imply that if the pilot stiffens his muscles, for example in response to an emergency, the feedthrough of lag regressive mode and lag progressive mode disturbances increases, causing a relative large amount of involuntary control inputs, which might aggravate the situation and can cause air resonance.

Fig. 10 shows the squared coherence for each condition, grouped per direction. The coherence found in the lateral direction is close to 1 for each frequency, indicating a reliable estimate was obtained. The coherences for the longitudinal direction are somewhat lower, especially for the PT, but are still regarded as acceptable. However, looking at the squared coherence for the PT in the vertical direction we see very low values, especially for the lower frequencies. The cause of this is most probably the limited motion space of the SIMONA simulator in the vertical direction (1.2m, 60% w.r.t. the lateral and longitudinal direction). Although a near maximum disturbance magnitude was used, the perturbations were apparently insufficient to obtain a high coherence between input and output. The consequence of this is that the BDFT estimate for the PT in vertical direction is not reliable, especially for the frequencies below 2 Hz. To obtain reliable results for the PT in vertical direction, the experiment would need to be done in a simulator with larger vertical motion space.

## 6. CONCLUSIONS

In this study BDFT was measured in a helicopter setup for three directions and for three control tasks. By measuring the admittance it was shown that the pilot adapted his neuromuscular system to each task. The results show that the BDFT dynamics vary both between subjects (intersubject variability), but more dominantly within a subject (intrasubject variability). The intrasubject

variability has been attributed to variations in the settings of the neuromuscular system.

Also, a dependency of disturbance axis was found. For the lower frequencies, up to 3-4 Hz, the level of BDFT is the highest in the lateral direction and the lowest in the vertical direction. From disturbances of 3-4 Hz and up the BDFT is the highest in the vertical direction.

By adding additional frequencies to the disturbance signal, the level of BDFT for three typical rotor modes was studied in more detail: the lag regressive mode (~2.96 Hz), flap coning mode (~7.56 Hz), and the lag progressive mode (~11.19 Hz). During the PT ('stiff' task) peaks in BDFT magnitude can be observed at 2-3 Hz, coinciding with the lag regressive mode, and at 11 Hz, coinciding with the lag progressive mode. This implies that if the pilot stiffens his muscles, for example in response to an emergency, the feedthrough of lag regressive mode and lag progressive mode disturbances increases, causing a relative large amount of involuntary control inputs, which might aggravate the situation and can cause air resonance.

From the squared coherence estimates it becomes clear that the magnitude of the motion disturbance signal for the position task in the vertical direction was insufficient to obtain reliable estimates of the BDFT up to 2 Hz. To obtain reliable results for the PT in vertical direction, the experiment would need to be done in a simulator with larger vertical motion space.

The method proposed in the current paper to measure admittance and BDFT has shown to yield reliable and repeatable results. The results of the study provide an insightful view in the occurrence of BDFT under different conditions for a large range of frequencies. By using the obtained BDFT dynamics as models, with realistic disturbance profiles as input, the level of BDFT can be simulated for a chosen flight condition.

For future research it would be interesting to investigate the occurrence of closed-loop effects, such as vertical bounce, where BDFT induced involuntary control inputs lead to helicopter accelerations that in turn cause involuntary inputs.

## 7. REFERENCES

- [1] McLeod, R.W., and Griffin, M.J., (1989) "Review of the effects of translational whole-body vibration on continuous manual control performance," *Journal of Sound and Vibration*, vol. 133, no. 1, pp. 55 – 115, 1989
- [2] Raney, D.L., Jackson, E.B., Buttrill, C.S. and Adams, W.M., (2001), "The impact of structural vibrations on flying qualities of a supersonic transport", *AIAA Atmospheric Flight Mechanics Conference*, 2001
- [3] Arai, F., Tateishi, J., and Fukuda, T., (2000), "Dynamical analysis and suppression of human hunting in the excavator operation", in *9th IEEE International Workshop on Robot and Human Interactive Communication, RO-MAN*, Osaka, Japan, pp. 394–399, 2000
- [4] Banerjee, D., Jordan, L.M., and Rosen, M.J., (1996), "Modeling the effects of inertial reactions on occupants of moving power wheelchairs," in *Proceedings of the Rehabilitation Engineering and Assistive Technology Society of North America Conference (RESNA)*, pp. 220–222, 1996

- [5] Mayo, J.R., (1989) "The involuntary participation of a human pilot in a helicopter collective control loop", *15th European Rotorcraft Forum*, Amsterdam, The Netherlands, September 12-15, 1989
- [6] Gabel, R., Wilson, G.J., (1968) "Test Approaches to External Sling Load Instabilities" *Journal of the American Helicopter Society*, 13 (3), pp. 44-54, 1968.
- [7] Allan, R.W., Jex, H.R., and Magdaleno, R.E. (1973), "Manual Control Performance and Dynamic Response during Sinusoidal Vibration", *AMRL-TR-73-78*, October 1973.
- [8] Magdaleno, R.E., Allen, R.W. and Jex, H. R., (1974), "Biodynamic Models for Vertical Vibration Interference on Pilot/Aircraft Pitch Control", Systems Technology Incorporated, *Technical Report No. 1037-1*, September 1974.
- [9] Ringland, R.F. and DiMarco, R.J., (1975), "Potential Bobweight Effects in the XV-15 Aircraft", Systems Technology, Inc., *WP 1048-6R*, November 1975.
- [10] Jex, H.R. and Magdaleno, R.E., (1978), "Biomechanical Models for Vibration Feedthrough to Hands and Head For a Semisupine Pilot", *Aviation, Space and Environmental Medicine*, Vol. 49, (1), January 1978.
- [11] McRuer, D.T., et al., (1997), "Aviation safety and pilot control. Understanding and Preventing Unfavorable Pilot-Vehicle Interactions", *ASEB National Research Council, National Academy Press*, Washington D.C., 1997
- [12] Parham, T. J., Popelka, D., Miller, D. G. and Frobel, A.T., (1991) "V-22 Pilot-In-The-Loop Aeroelastic Stability Analysis", *American Helicopter Society 47th Annual Forum*, Phoenix, AZ, May 1991
- [13] Kaplita, T.T., Driscoll J.T., Diftler, M.A., Hong, S. W., (1989), "Helicopter Simulation Development by Correlation with Frequency Sweep Flight Test Data", *American Helicopter Society 45th Annual Forum*, Boston, MA, May 1989
- [14] Ingle, S.J., Weber, T.L., and Miller, D.G., (1994), "Concurrent Handling Qualities and Aero-servoelastic Specification Compliance for the RAH-66 Comanche", *American Helicopter Society Aeromechanical Specialist Conference*, San Francisco, California, January 1994
- [15] Dieterich, O., Götz, J., DangVu, B., Haverdings, H., Masarati, P., Pavel, M.D., Jump, M., and Gennaretti, M. (2008) "Adverse Rotorcraft-Pilot Coupling: Recent Research Activities in Europe", *34th European Rotorcraft Forum*, Liverpool, UK, , September 16-19, 2008.
- [16] Mattaboni, M., Quaranta, G, Masarati, P., and Jump, M. (2008) "Experimental Identification of Rotorcraft Pilots' Biodynamic Response for Investigation of PAO Events", *34th European Rotorcraft Forum*, Liverpool, UK, September 16-19, 2008
- [17] Masarati, P., Quaranta, G., Basso, W., Bianco-Mengotti, R., and Monteggia, C. (2009) "Biodynamic tests for pilots' characterization on the BA-609 fly-by-wire tiltrotor", *XX Italian Association of Aeronautics and Astronautics (AIDAA) Congress*, Milano, Italy, June 29-July 3, 2009
- [18] Sövényi, S. and Gillespie, R.B. (2007). "Cancellation of biodynamic feedthrough in vehicle control tasks". *IEEE Transactions On Control System Technology*, 15 (6), pp. 1018- 1029, 2007.
- [19] Venrooij, J., Abbink, D.A., Mulder, M., van Paassen, M.M., and Mulder, M. (2010) "Biodynamic feedthrough is task dependent", *IEEE International Conference on Systems, Man, and Cybernetics - SMC 2010*, Istanbul, Turkey, October 10-13, 2010,
- [20] Venrooij, J., Abbink, D.A., Mulder, M., van Paassen, M. M., and Mulder, M., (2011), "A method to measure the relationship between biodynamic feedthrough and neuromuscular admittance," *IEEE Transactions on Systems, Man, and Cybernetics, Part B: Cybernetics*, vol.PP, no.99, pp.1-12, 2011.
- [21] Stroosma, O., van Paassen, M.M., and Mulder, M. (2008), "Using the SIMONA research simulator for human-machine interaction research," *Proceedings of the AIAA Modeling and Simulation Technologies Conference and Exhibit*, Austin, Texas, 2008
- [22] Mitchell, D.G. , Hoh, R.H. , Adolph, Jr., A, and Key, D., (1992) "Ground Based Simulation Evaluation of the Effects of Time Delays and Motion on Rotorcraft Handling Qualities", *USAAVSCOM TR 91-A-010, AD-A256 921*, Jan. 1992
- [23] Abbink, D.A., (2006), "Neuromuscular analysis of haptic gas pedal feedback during car following." *Ph.D. dissertation*, Delft University of Technology, 2006.
- [24] Perreault, E.J. Kirsch, R.F. and Crago, P.E., (2001), "Effects of voluntary force generation on the elastic components of endpoint stiffness," *Experimental Brain Research*, vol. 141, pp. 312–323, 2001.
- [25] Schouten, A.C., de Vlugt, E. and van der Helm, F. C.T., (2008), "Design of perturbation signals for the estimation of proprioceptive reflexes," *IEEE Trans. Biomed. Eng.*, vol. 55, no. 5, pp. 1612 – 1619, 2008.
- [26] Williams, J.N., Ham, J.A, Tischler, M.B., (1995), "Flight Test Manual – Rotorcraft Frequency Domain Flight Testing", *U.S. Army Aviation Technical Test Center, AQTD: Project No. 93-14*, CA, Sep. 1995
- [27] Walden, R.B., (2007), "A Retrospective Survey of Pilot-Structural Coupling Instabilities in Naval Rotorcraft", *63rd Annual Forum of the American Helicopter Society*, Virginia Beach, VA, May 1-3, 2007
- [28] Aponso, B.L., Johnston, D.E., Johnson, W.A., Magdaleno, R.E., (1994), "Identification of Higher Order Helicopter Dynamics Using Linear Modeling Methods" *Journal of the American Helicopter Society*, Vol. 39, No 3, July 1994.
- [29] Curtiss H.C. Jr, (1994), "Comment on 'Identification of Higher Order Helicopter Dynamics Using Linear Modeling Methods'", *Journal of The American Helicopter Society*, vol. 39, no. 3, 1994
- [30] Mugge, W., Abbink, D.A. and van der Helm, F. C.T. (2007), "Reduced power method: how to evoke low-bandwidth behaviour while estimating full-bandwidth dynamics," in *IEEE 10th International Conference on Rehabilitation Robotics. ICORR 2007*, pp. 575 – 581, 2007
- [31] van der Helm, F.C.T., Schouten, A.C., de Vlugt, E. and Brouwn, G.G., (2002), "Identification of intrinsic and reflexive components of human arm dynamics during postural control," *Journal of Neuroscience Methods*, vol. 119, pp. 1–14, 2002.